Submitted to Metallurgical Transactions

LBL-824
Preprint

FLUID FLOW IN A PROPAGATING CRACK

John Newman and William H. Smyrl

April 1972

Prepared for the U. S. Atomic Energy Commission
under Contract W-7405-ENG-48

DISCLAIMER

 LBL-824

Fluid Flow in a Propagating Crack

John Newman

Inorganic Materials Research Division,
Lawrence Berkeley Laboratory, and
Department of Chemical Engineering;
University of California, Berkeley

and

William H. Smyrl*

Boeing Scientific Research Laboratories,
Seattle, Washington

April 1972

Abstract

The fluid flow in a sharp, propagating crack is shown to have a large pressure drop near the tip for finite crack velocities. An analysis of the effect of liquid surface tension is made to determine the possibility of cavitation of the liquid. The analysis indicates that cavitation is possible for certain liquid metal embrittlement systems. Other systems apparently cannot support cavitation, but the fluid flow will still be important since it influences mass transport within the propagating crack.

---

*Present address: Sandia Laboratories, Albuquerque, New Mexico

Introduction

Stress corrosion cracking, or environmentally-induced, sub-critical crack growth, occurs in a wide range of materials and a wide range of environments. In titanium alloys, for example, cracking has been observed in a number of gaseous, liquid, and solid environments. However, if one takes a single titanium alloy, in a single heat treatment condition, and examines crack propagation as a function of the mechanical variable, the crack-tip stress intensity, for different liquid environments, a common pattern emerges (1). That is, in many environments the velocity (v_I) at low values of the stress intensity is exponentially dependent on the stress intensity, but becomes independent (v_{II}) of it at higher values of the stress intensity. The process which limits the velocity v_{II} is the subject of interest in this paper.

Although there is this common pattern which is observed in many environments, the absolute magnitude of the velocity at a particular stress intensity varies widely for different liquids. v_{II} is 40 cm/sec in liquid mercury, 1 cm/sec in LiCl-KCl eutectic at 375° C, 5×10^{-2} cm/sec in 10 M aqueous HCl, 4×10^{-3} cm/sec in CCl_4, and 6×10^{-5} cm/sec in methanol* (1). Therefore, one has the task of explaining not only the existence of a plateau velocity for each environment, but also why it varies so much for the different liquids. We shall adopt the assumption for the purposes of this paper, that a similar process is responsible for the plateau velocity in each liquid. The fluid flow phenomena which should be common for all these systems will be treated here.

---

*Note: These data are for Titanium-8% aluminum-1% Molybdenum-1% Vanadium in the mill-annealed condition at 24°C, except as otherwise noted.

Rostoker, et al. (2) have reviewed the data on liquid metal embrittlement. They have proposed a semi-quantitative theory which accounts for the limiting crack velocity by considering fluid flow processes in the crack. Rhines, et al. (3) interpret their results as indicating that liquid metal embrittlement is controlled by the flow of the liquid metal to the crack tip. Robertson (4) has discussed the possibility of a dissolution process limiting the crack propagation of liquid metal embrittlement, without specifically introducing the influence of fluid flow. Beck and Grens (5) have proposed a mass transport-kinetic model for stress corrosion cracking in aqueous electrolytic solutions. The adsorption theory, various brittle-film theories, and the ubiquitous hydrogen theory are only qualitative and have been reviewed elsewhere (1,6), so they will not be considered further here. Fluid flow in the propagating crack is mentioned in some way, although sometimes in a minor role, in each of the four papers above. It is not fully treated in a quantitative way for a realistic crack geometry in any of them, however. This situation led to the study of hydrodynamic phenomena which should occur in a propagating crack, as a contribution toward the general effort of understanding stress corrosion cracking. In particular, we study the flow behavior in a crack propagating in a material with a planar crack front, and in which the crack extends completely through the thickness of the material.

Mathematical Formulation

A crack propagating into a material, as in stress corrosion cracking, will tend to draw the fluid in behind it, as sketched in figure 1 in a coördinate system in which the crack tip is stationary. In this coördinate system, the walls of the crack appear to move with a velocity V, and the process is time independent. The fluid in the crack is assumed to be an incompressible, Newtonian liquid of constant viscosity.

We shall analyze the velocity and pressure distributions in such a crack, ignoring any mass transfer or deviations from an ideal crack geometry. These distributions are determined by the Navier-Stokes momentum equation,

$$\underline{v}\cdot\nabla\underline{v} = -\frac{1}{\rho}\nabla\mathcal{P} + \nu\nabla^2\underline{v} \quad , \tag{1}$$

and the continuity equation for a material of uniform density,

$$\nabla\cdot\underline{v} = 0 \quad . \tag{2}$$

These equations are written out in cylindrical coördinates in the text of Bird, Stewart, and Lightfoot (7). Moffatt (8) has applied these equations to the general problem of fluid flow near corners.

In solving the problem, we have used a dimensionless stream function ψ, which yields the velocity components as

$$v_r = -\frac{\nu}{r}\frac{\partial\psi}{\partial\theta} \quad \text{and} \quad v_\theta = \nu\frac{\partial\psi}{\partial r} \quad . \tag{3}$$

In this manner, the continuity equation 2 is identically satisfied. For economy of parameters, we also use a dimensionless radial distance R from the crack tip:

$$R = rV/\nu \quad . \tag{4}$$

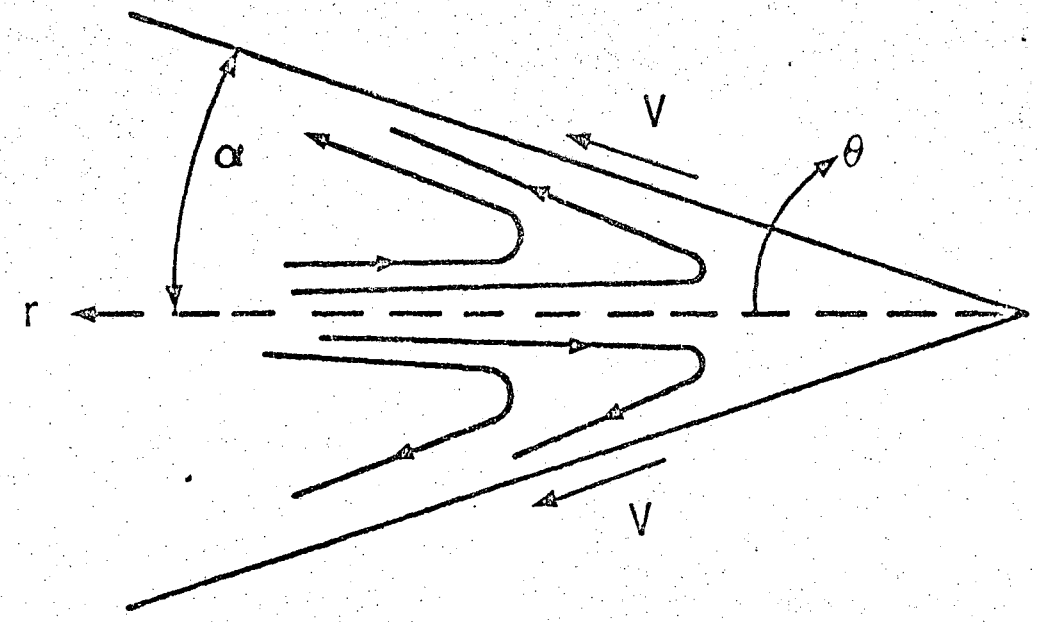

FIGURE 1. FLUID FLOW IN A PROPAGATING CRACK

The dynamic pressure $\mathcal{P}$ can be eliminated between the two components of the momentum equation 1. The resulting fourth-order differential equation for ψ can be expressed as

$$\frac{1}{R}\left(\frac{\partial\psi}{\partial R}\frac{\partial\omega}{\partial\theta} - \frac{\partial\psi}{\partial\theta}\frac{\partial\omega}{\partial R}\right) = \frac{\partial^2\omega}{\partial R^2} + \frac{1}{R}\frac{\partial\omega}{\partial R} + \frac{1}{R^2}\frac{\partial^2\omega}{\partial\theta^2} \quad , \tag{5}$$

where

$$\omega = \frac{\partial^2\psi}{\partial R^2} + \frac{1}{R}\frac{\partial\psi}{\partial R} + \frac{1}{R^2}\frac{\partial^2\psi}{\partial\theta^2} \tag{6}$$

is a dimensionless vorticity. The boundary conditions are

$$\psi = 0 \quad \text{at} \quad \theta = \pm\alpha \quad , \tag{7}$$

$$\partial\psi/\partial\theta = -R \quad \text{at} \quad \theta = \pm\alpha \quad , \tag{8}$$

where 2α is the crack angle (see figure 1). These conditions say that $v_r = V$ and $v_\theta = 0$ at the crack walls. Condition 7 also says that there is no net flow into the crack. The conditions at $\theta = -\alpha$ can be replaced by the symmetry condition; ψ is an odd function of θ.

In the dimensionless form of the problem, there are no parameters except the crack angle. The procedure is to solve equation 5 for the stream function ψ. This is equivalent to determining the velocity components v_r and v_θ. The dynamic pressure, in the dimensionless form $\mathcal{P}/\rho V^2$, can then be obtained, except for an additive constant, from equation 1.

A term like the Reynolds number appears only in the dimensionless independent variable $R = rV/\nu$. Hence, it is appropriate to seek solutions for large and for small values of R.

Solution near the crack tip

Near the crack tip it should be possible to neglect the inertial terms in the equation of motion (i.e., $\underline{v}\cdot\nabla\underline{v}$ or the left side of equation 5). On this basis, the stream function can be expanded in a power series in R:

$$\psi = R\sum_{k=0}^{\infty} R^k \psi_k(\theta) \quad . \tag{9}$$

Substitution into equation 5 shows that ψ_o satisfies

$$\psi_o^{iv} + 2\psi_o'' + \psi_o = 0 \tag{10}$$

and ψ_1 satisfies

$$\psi_1^{iv} + 4\psi_1'' = [\psi_o(\psi_o+\psi_o'')]' \quad , \tag{11}$$

thus accounting for the inertial terms neglected in obtaining equation 10. The solutions are

$$\psi_o = A \sin\theta + B\theta\cos\theta \tag{12}$$

and

$$\psi_1 = C \sin 2\theta + D\theta + \left(\frac{3B^2}{32} - \frac{AB}{8}\right)\theta\cos 2\theta + \frac{B^2}{16}\theta^2 \sin 2\theta \quad , \tag{13}$$

where

$$A = \frac{-\alpha \cos \alpha}{\alpha - \cos \alpha \sin \alpha} \quad , \quad B = \frac{\sin \alpha}{\alpha - \cos \alpha \sin \alpha} \quad , \tag{14}$$

$$\left.\begin{aligned} C &= \frac{B}{8} \frac{(B-2A)\alpha^2 \sin 2\alpha - B\alpha^3 \cos 2\alpha}{2\alpha \cos 2\alpha - \sin 2\alpha} \quad , \\ D &= \frac{B}{32} \frac{4B\alpha \sin^2 2\alpha + (4A-3B)(2\alpha - \cos 2\alpha \sin 2\alpha)}{2\alpha \cos 2\alpha - \sin 2\alpha} \quad . \end{aligned}\right\} \tag{15}$$

Equations 12 and 13 can be used with equation 3 and substituted into either the r or the θ component of the equation of motion 1 to yield an ordinary differential equation for the dynamic pressure. Integration of the resulting equation yields

$$\frac{\mathcal{P}}{\rho V^2} = -\frac{2B}{R} \cos \theta - (AB + 4D) \ln R + \text{const} + O(R) \quad . \tag{16}$$

The first term on the right is due to ψ_o, while ψ_1 contributes the term in ln R. Higher order terms in ψ contribute the terms of O(R) in this equation.

In the region near the tip of the crack, the two velocity components are of order V, and the dynamic pressure is of order $\mu V/r$. The dynamic pressure approaches minus infinity at the crack tip. This means that the liquid cannot easily fill the void behind the propagating crack. Therefore, "cavitation" might be expected to occur near the crack tip.

Solution far from the crack tip

For large values of αR, the viscous terms in equation 1 should be negligible compared to the inertial terms, except in a thin boundary layer near the wall. Within the boundary layer, that is near the crack walls, ψ is given, to a first approximation, by

$$\psi = R^{1/2} F(Y) \quad , \tag{17}$$

where

$$Y = R^{1/2}(\alpha-\theta) = \left(\frac{rv}{\nu}\right)^{1/2}(\alpha-\theta) \quad . \tag{18}$$

The function F is to be determined by substitution of (17) and (18) into equation 5. It is found that F satisfies

$$F^{iv} + \frac{1}{2}FF''' + \frac{1}{2}F'F'' = 0 \quad . \tag{19}$$

The exponent on R in equation 18 is dictated by the requirement that one of the viscous terms be included in equation 19. Otherwise, equation 19 would be a third order equation, and all the boundary conditions could not be satisfied.

The exponent on R in equation 17 is dictated by boundary condition 8. Boundary conditions on F thus are

$$F = 0 \ , \ F' = 1 \ \text{ at } \ Y = 0 \quad . \tag{20}$$

In addition, F must match the solution outside the boundary layer. This would appear to require that F approach a constant for large values of Y. Thus, we write

$$F' \to 0 \quad \text{as} \quad Y \to \infty \quad . \tag{21}$$

Integration of equation 19 yields

$$F''' + \frac{1}{2}FF'' = \text{constant} = 0 \quad , \tag{22}$$

where the integration constant is set equal to zero according to condition 21. The solution for F was obtained numerically (14) and is shown in figure 2. From these results we find that

$$F''(0) = -0.445748 \tag{23}$$

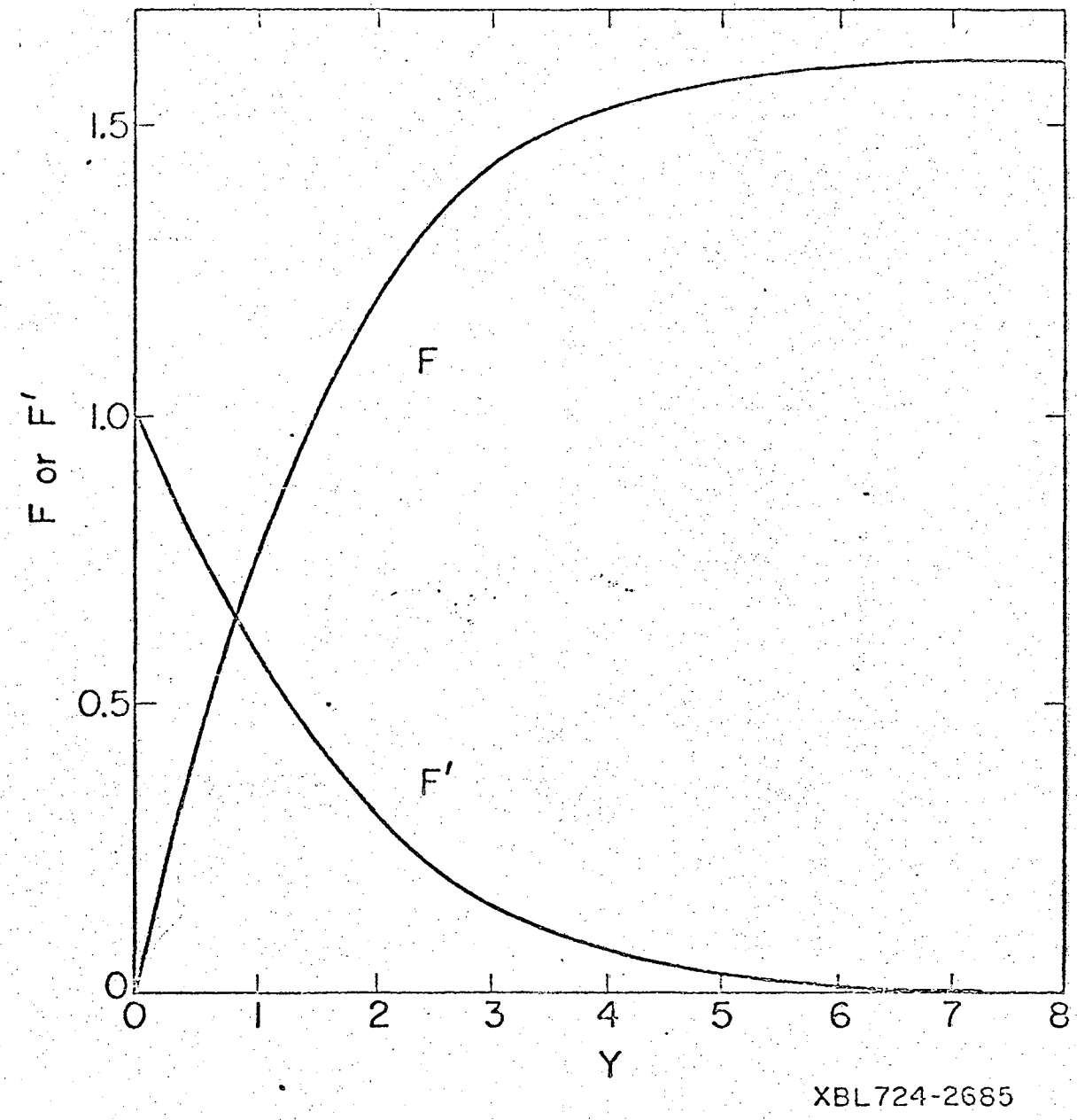

Figure 2. The boundary-layer function F, and its first derivative F', as a function of the position variable Y.

and

$$F(\infty) = 1.616125 \quad . \tag{24}$$

Outside the boundary layer, ψ takes the form

$$\psi = 2R^{1/2} g(\theta) \quad , \tag{25}$$

this being a first approximation for large values of R. The exponent on R is dictated by the requirement that, as θ approaches α, this solution must match the boundary-layer solution. Substitution into equation 5 shows that g satisfies the equation

$$gg''' + 3g'g'' + gg' = 0 \quad . \tag{26}$$

Integration gives

$$gg'' + (g')^2 + \frac{1}{2}g^2 = K^2 \quad . \tag{27}$$

Since ψ is odd in θ, boundary conditions are

$$g = g'' = 0 \quad \text{at} \quad \theta = 0 \quad . \tag{28}$$

Thus, $g' = K$ at $\theta = 0$. Let us define a new function G by

$$g = KG \quad , \tag{29}$$

so that

$$\psi = 2R^{1/2} KG(\theta) \quad . \tag{30}$$

in the region outside the boundary layer.

Then G satisfies

$$GG'' + G'G' + \frac{1}{2}G^2 = 1 \quad , \tag{31}$$

$$G = 0 \quad , \quad G' = 1 \quad \text{at} \quad \theta = 0 \quad . \tag{32}$$

The problem for G can be solved directly; the results are given in table 1. The power-series expansion is

$$G = \theta - \frac{\theta^3}{24} + \frac{\theta^5}{1920} + O(\theta^7) \quad . \tag{33}$$

For the crack angles of interest, G does not differ significantly from θ.

The constant K is determined by matching the solution 30 with the boundary-layer solution 17, with the result

$$2KG(\alpha) = F(\infty) \quad . \tag{34}$$

Substitution of equation 30 into equation 1 shows that, outside the boundary layer, the dynamic pressure varies as

$$\frac{\mathscr{P}'}{\rho V^2} = -\frac{2K^2}{R} + \text{constant} \quad . \tag{35}$$

The dependence on R is the same in this region as it is near the crack tip (see equation 16); consequently, the coefficients K^2 and B are compared in table 1. Since for large R, the pressure variation is proportional to K^2/R and, for small R, proportional to B/R (at $\theta = 0$), it is reasonable to ask how well these two expressions "match" at intermediate values of R.

Table 1. Values of the functions G, α^2K^2, and α^2B for different values of the crack angle.

α	$G(\alpha)$	α^2K^2	α^2B
0	0	0.65296	1.5
0.1	0.09996	0.65351	1.5005
0.2	0.19967	0.65515	1.5020
0.3	0.29888	0.65788	1.5045
0.4	0.39734	0.66174	1.5078
0.5	0.49481	0.66674	1.5121
0.6	0.59104	0.67291	1.5171
0.7	0.68580	0.68029	1.5229
0.8	0.77884	0.68893	1.5293
0.9	0.86993	0.69888	1.5360
1.0	0.95885	0.71021	1.5430

The fact that they differ by about a factor of 2 indicates that there is still a third, intermediate region between the crack-tip region and the region far from the crack tip. This intermediate region is not vitally important here since, from the present treatment, we know the pressure everywhere to within a factor of 2, and usually better, which is adequate for the discussion. For any values of α in the table, it is easy to compare K^2 and B. These are tabulated as α^2K^2 and α^2B in order to draw attention to the fact that the dependence on the crack angle is nearly the same; K^2 and B are both approximately inversely proportional to the square of α.

Discussion

Except near the walls, the fluid flow characteristics in the outer part of the crack are determined by a balance between inertia and the pressure force. Nearer the crack tip and at the walls, viscous forces become important, and very near the crack tip the viscous and pressure forces are dominant. Phenomena near the crack tip which are sensitive to the fluid flow will then be dependent on the viscosity and the local pressure of the fluid. Velocity profiles for the tip region can be calculated from equations 3, 9, 12, and 13. In the outer part of the crack, equations 17 and 30, figure 2, and table 1 can be used to calculate the velocity profiles. These velocity profiles can be used, for example, to calculate concentration profiles and mass-transfer behavior in a propagating crack. Thus, even if the fluid flow is not found to control directly the velocity of cracking, the hydrodynamics will still be important for the complete description of events occurring in the crack.

An idealized situation has been treated in the theoretical development. In a propagating crack, the viscosity and density will depend upon the local composition and temperature, and eventually the finite thickness of the material will have to be accounted for. Thus, fluid need not come in only from large values of r; there will also be seepage from the edge of the crack, and this will become dominant for large values of r, where αr is not small compared with the thickness of the specimen.

Fluid flow could control the velocity of cracking as the result of cavitation. Cavitation would interrupt the fluid flow to the tip, preventing further extension of the crack until the crack slowed

down to permit collapse of the cavity. The balance between propagation and incipient cavitation would seem to require a characterisitic velocity which could not be exceeded, but below which no cavitation would occur. An analysis is presented below of the possibility of cavitation in the fluid. This is a highly idealized model where the surface tension effects in the liquid are viewed as preventing or retarding cavitation, whereas the pressure drop due to the fluid flow is acting to produce cavitation. We first calculate the pressure inside and outside a bubble enclosed in the crack. The required pressure outside the bubble is then compared to the pressure due to the fluid flow to determine whether this required pressure is available from the fluid flow. We consider the fluid to fill completely the crack before any bubble formation, since for the systems analyzed, the liquid apparently completely "wets" the solid. The model depicted in Figure 3 will be referred to in the discussion to follow.

Equilibrium pressure near a bubble

The thermodynamic stability of a cavitation bubble is governed by its size and surface tension. The vapor pressure of the liquid is lowered by surface-tension effects, as given by the Kelvin equation

$$\frac{\tilde{V}_{liq}}{RT}(p_e - p_o) = \ell n(\frac{p_i}{p_o}) \quad . \tag{36}$$

The relationship between the pressure inside and outside the bubble is given by the Laplace equation,

$$p_i - p_e = \frac{\sigma}{r_o} \quad . \tag{37}$$

From a knowledge of the normal vapor pressure p_o of the liquid over a planar surface, the molar volume $\tilde{V}_{liq}$ of the liquid, and the surface tension σ, these two equations permit the calculation of the pressure inside and outside a cylindrical bubble whose radius of curvature is

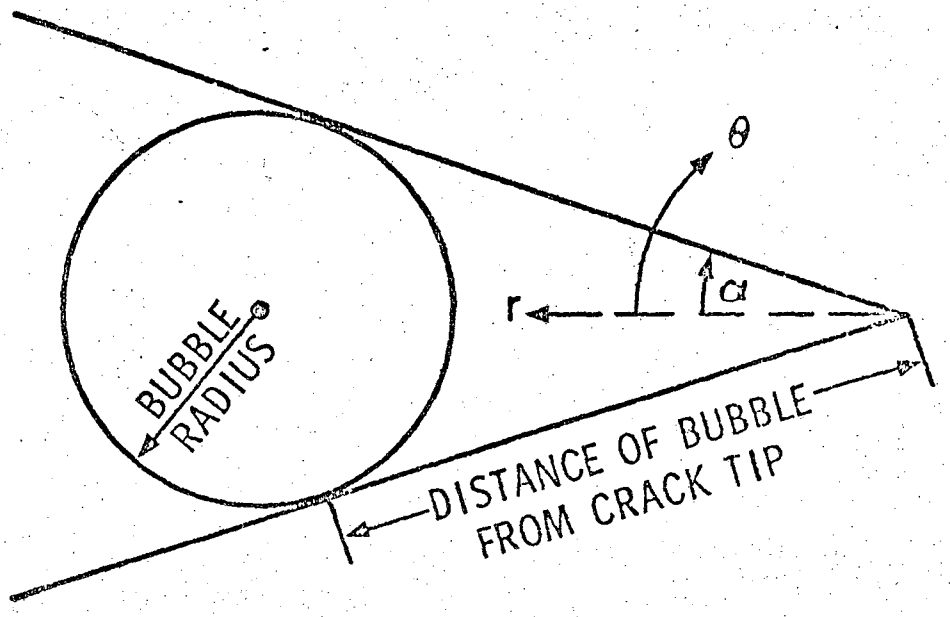

PRESSURE OUTSIDE BUBBLE IS p_e

PRESSURE INSIDE BUBBLE IS p_i

FIGURE 3. MODEL FOR BUBBLE INSIDE CRACK

r_o. In table 2 below are results of such a calculation for mercury.* It should be noted immediately that the pressure outside a bubble of small radius may be negative. The bubble was taken to be a cylinder with its axis perpendicular to the plane defined by the coördinate system of figure 1 (see figure 3).

Pressure in a propagating crack

For a given distance from the crack tip, the largest bubble that could be enclosed would have its diameter equal to the crack opening at this distance. Since the crack opening is approximately equal to $2\alpha r$ for small crack angles, a given bubble diameter establishes the minimum distance from the crack tip that it could be located. Using the bubble radii in table 2, the dimensionless distance from the mercury crack tip in Ti 8-1-1 is given in table 3,** for a crack angle 2α = 0.2 degree = 0.00349 radian. Also given in this table is the pressure distribution in a propagating mercury crack in Ti 8-1-1. For values of R greater than 1.5×10^7 (or $\alpha^2 R$ greater than 47), equation 35 was used to calculate the pressure, with a value of the constant of 46.189, evaluated by assuming p goes to 1 bar at $R = \infty$.

---

*The physical properties of mercury, obtained from the Handbook of Chemistry and Physics (10), are p_o = 2.46 dyne/cm^2, $\tilde{V}_{liq}$ = 14.8227 cm^3/mole, σ = 484 dyne/cm.

**The kinematic viscosity of mercury was taken to be 1.12×10^{-3} cm^2/sec (10). Recall that the plateau cracking velocity is 40 cm/sec in liquid mercury.

Table 2. Dimensionless pressure inside and outside a vapor bubble in liquid mercury, 25°C, and the pressure outside the bubble

r_o(cm)	p_i/p_o	p_e/p_o	p_e(bar)
∞	1	1	2.43×10^{-6}
10^{-3}	0.99971	-1.967×10^{5}	-0.478
10^{-4}	0.9971	-1.967×10^{6}	-4.776
10^{-5}	0.971	-1.967×10^{7}	-47.76
10^{-6}	0.748	-1.967×10^{8}	-477.6
10^{-7}	0.055	-1.967×10^{9}	-4776

Table 3. Pressure distribution in a propagating mercury crack in Ti 8-1-1.

bubble radius ($=\alpha r$) (cm)	R ($= \frac{rV}{\nu}$)	p (bar)
10^{-3}	2.05×10^{4}	-0.016
10^{-4}	2.05×10^{3}	-9.36
10^{-5}	2.05×10^{2}	-102.9
10^{-6}	20.5	-1038.3
10^{-7}	2.05	-10,393

Table 4. Cracking velocity, surface tension, viscosity, and resulting maximum crack angle at which cavitation is still possible.

Liquid	V cm/sec	σ dyne/cm	μ g/cm-sec	$2\alpha_{max}$ deg
Hg	40	484	0.01554	0.44
LiCl-KCl	1	150	0.02	0.046
10 M HCl	5×10^{-2}	67.4	0.0163	0.0042
CCl_4	4×10^{-3}	26.95	0.00969	4.9×10^{-4}
CH_3OH	6×10^{-5}	22.61	0.00597	5.4×10^{-6}

For R less than 1.5×10^7, equation 16 was used to calculate the pressure, assuming the constant is of the order of 49, to match with equation 35 at $R = 1.5 \times 10^7$.

Conditions for cavitation

Comparison of the pressure in table 3 with p_e in table 2 indicates that it is possible to generate a cavitation bubble in these cracks. If one changes the crack angle to 0.4° (from 0.2°), the calculated pressure in table 3 is decreased by a factor of roughly two, and it is still just small enough to make cavitation possible.

Figure 4 illustrates graphically the values of the pressure required to produce a given size bubble in relationship to the pressure predicted by the hydrodynamics at a corresponding position in the crack ($\alpha r = \ddot{r}_o$). For small values of r_o, equations 36 and 37 yield a curve with a slope of $-\sigma$. The hydrodynamic curve has a slope of $-2B\mu V\alpha$ if we evaluate equation 16 on the crack centerline. In order for cavitation to be possible, these two curves must intersect, and the position of the intersection would indicate the largest possible bubble. The limiting case would be where the two curves are nearly parallel. A necessary condition for bubble formation would then be simply

$$\sigma \leq 2B\mu V\alpha.$$

Since the other variables are already known, we should like to express this as a condition on the crack angle. In order for cavitation to be possible, we must have

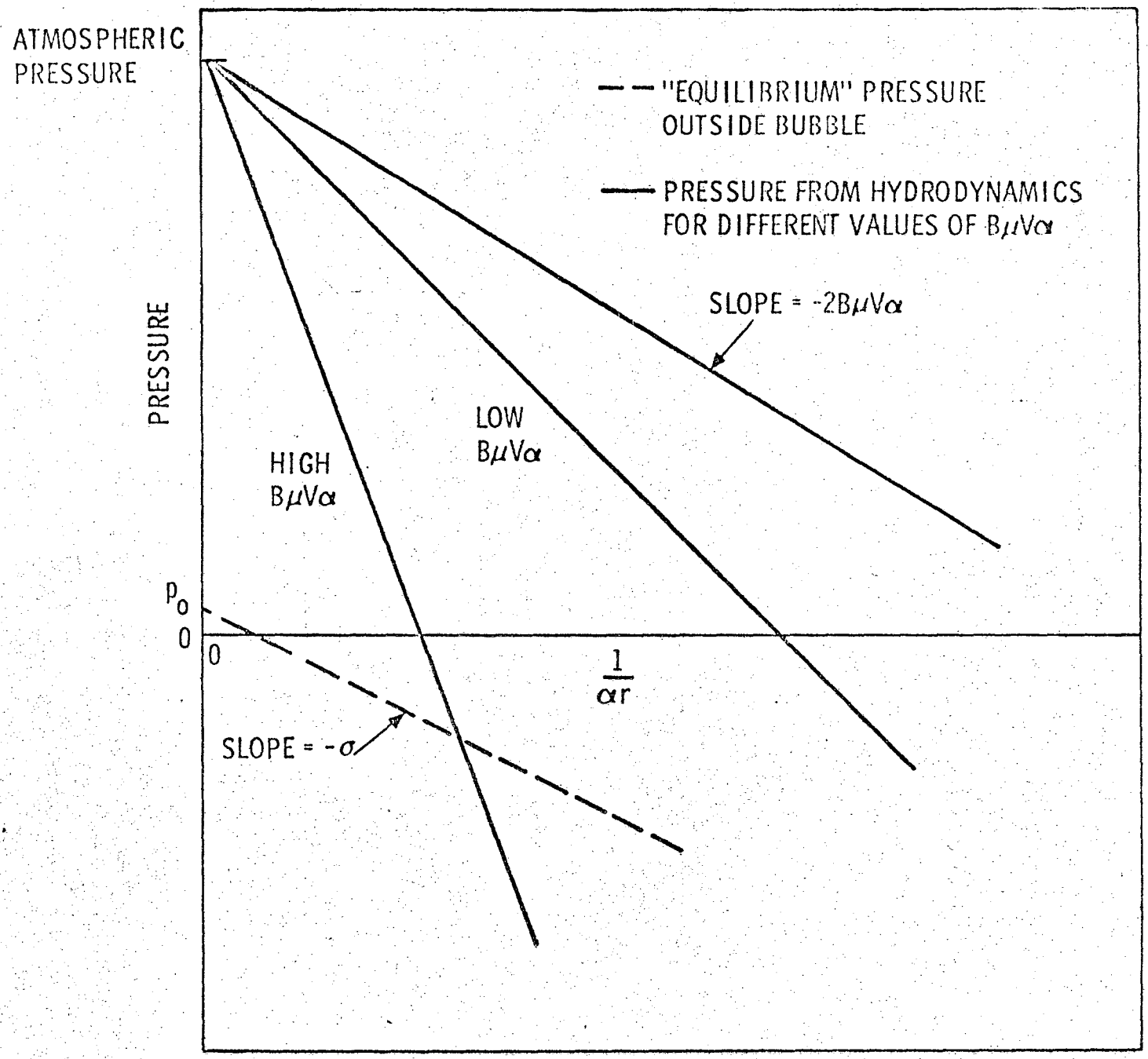

FIGURE 4. PRESSURE FROM HYDRODYNAMICS COMPARED TO EQUILIBRIUM PRESSURE OUTSIDE CAVITATION BUBBLE

$$\alpha \leq 3\mu V/\sigma \qquad (38)$$

(the numerical factor 3 being the limiting value of $2B\alpha^2$ for small crack angles). For larger values of α, no intersection of the curves will be found on figure 4. Since α is often too small to be measured conveniently, this criterion provides an estimate of α (see table 4). If α, μ, and σ are known for a given system, this condition provides a lower bound for the plateau cracking velocity if cavitation is to be an important mechanism for limiting crack propagation. On this basis the plateau cracking velocity should be relatively independent of the external pressure. The wide range of values of the maximum crack angle for the several liquids in table 4 suggests that some other mechanism besides cavitation is limiting the crack velocity for methanol and carbon tetrachloride.

Effect of blunting of the crack

Geometrical changes in the crack shape could have an important effect on the fluid flow. It is considered outside the scope of this paper to consider other geometries exhaustively, but the "rounding" effect of plastic deformation will be considered qualitatively. This effect can be seen most easily for a hyperbolic-shaped crack tip, where the amount of "rounding" may be characterized by the distance from the vertex of

the hyperbola to the intersection of the asymptotes. Equations 9 and 16 are still approximately valid for the region of space filled with the liquid and one concludes that cavitation might be prevented below a certain characteristic velocity. That is, if one concluded on the basis of the sharp crack calculation that cavitation might be possible and the cavitation were expected to occur too near the crack tip, the effect of rounding might prevent it.

These calculations have served only to determine the possibility of cavitation in propagating cracks, and nothing has been said about the probability of the nucleation of vapor bubbles. Such a discussion is considered to be outside the scope of this paper. Also neglected have been such interesting points as the movement of liquid around a bubble (i.e., would liquid move toward or away from the crack tip?), the direction of movement of the bubble itself, and the mechanism of collapse of the bubble. All these points would require the treatment of entirely new fluid mechanics problems, and this is not considered to be appropriate at the present time. Also, we have not assessed the importance of the limiting negative pressure that a liquid may sustain, but several authors have discussed this for other systems (11, 12, 13).

The present treatment may be compared to that of Rostoker, et.al., (2)(see also Perrone and Liebowitz (15)), which was made on a cylindrical crack. Their procedure is much the same as that used here, that is, the pressure to generate a bubble of radius r is assumed to be given by the fluid mechanics of Poiseuille flow. The primary difficulty with this model is that it does not indicate any preferred distance from the crack tip where cavitation would be likely to occur. Indeed, cavitation could

occur anywhere along the cylinder by their model, if the velocity of crack propagation were fast enough. This should be contrasted with the present calculations where cavitation would become increasingly likely as the crack tip is approached, if the inequality (38) is obeyed. Also, they did not consider the details of the fluid flow near the apex of the cylinder (crack tip), but this region would probably be the most important. The fluid flow near the crack tip would be expected to be modified from the Poiseuille flow far from the crack tip.

The question of whether or not cavitation occurs during crack extension is important and should be investigated by experimental means. This could possibly be done by sonic or ultrasonic techniques. One critical test would be to conduct such tests in materials under mechanical fracture conditions where the velocity of cracking may approach approximately one-third the speed of sound.

Conclusions

The fluid flow in a sharp, propagating crack is shown to produce cavitation in the fluid near the crack tip, at finite crack velocities. For crack shapes which differ by having "rounded" tips, one may have cavitation only above certain crack velocities. These fluid flow results would be important in the calculation of mass-transport phenomena.

Acknowledgment

This work was supported by the United States Atomic Energy Commission and by the Boeing Company.

Notation

A,B,C,D	constants in solution for stream function near the crack tip
F	dimensionless function for stream function in boundary layer
g	dimensionless function for stream function outside boundary layer
G	dimensionless function for stream function outside boundary layer
K	integration constant in solution for stream function outside boundary layer
p_e	pressure external to bubble of radius r_o (dyne/cm^2)
p_i	pressure inside bubble of radius r_o (dyne/cm^2)
p_o	equilibrium vapor pressure over a plane surface (dyne/cm^2)
$\mathcal{P}$	dynamic pressure in fluid (dyne/cm^2)
r	radial distance from crack tip (cm)
r_o	radius of cylindrical bubble (cm)
R	dimensionless radial distance from crack tip
R	universal gas constant (8.3143 J/mole-deg)
T	absolute temperature (degrees Kelvin)
$\underline{v}$	fluid velocity (cm/sec)
v_I	crack tip velocity in Region I (cm/sec)
v_{II}	crack tip velocity in Region II (cm/sec)

V	wall velocity in coordinate system such that crack tip is stationary (cm/sec)
$\bar{V}$	molar volume (cm^3/mole)
2α	crack angle (radian)
θ	angular distance from crack center line (radian)
ν	fluid kinematic viscosity (cm^2/sec)
ρ	fluid density (g/cm^2)
σ	surface tension (dyne/cm)
ψ	dimensionless strean function
ω	dimensionless vorticity
μ	fluid viscosity (gm/cm-sec)

References

1. M. J. Blackburn, J. A. Feeney, and T. R. Beck, Advances in Corrosion Science and Technology, vol. 3, M. G. Fontana, R. W. Staehle, Eds., Plenum Press, New York, 1973.
2. W. Rostoker, J. M. McCaughey, and H. Markus, Embrittlement by Liquid Metals, Reinhold, New York, 1960.
3. F. N. Rhines, J. A. Alexander, and W. F. Barclay, Trans.ASM, 1962, vol. 55, pp. 22-44.
4. W. M. Robertson, Trans.TMS-AIME, 1966, 236, pp. 1478-1481.
5. T. R. Beck and E. A. Grens, J.Electrochem.Soc., 1969, 116, pp. 177-184.
6. M. O. Speidel and M. V. Hyatt, Advances in Corrosion Science and Technology, vol. 2, M. G. Fontana, R. W. Staehle, Eds., Plenum Press New York, 1972.
7. R. Byron Bird, Warren E. Stewart, and Edwin N. Lightfoot, Transport Phenomena, John Wiley and Sons, Inc., New York, 1960.
8. H. K. Moffatt, J.Fluid Mech., 1964, 18, pp. 1-18.
9. G. I. Taylor, J.Fluid Mech., 1963, 16, pp. 595-619.
10. Handbook of Chemistry and Physics 52nd Edition, The Chemical Rubber Company, Cleveland, Ohio, 1971-72.
11. A. T. J. Hayward, American Scientist, 1971, 59, pp. 434-443.
12. H. N. V. Temperely, Proc.Phys.Soc., 1947, 59, pp. 199-208.
13. R. D. Preston, pp. 366-378, in The Structure and Properties of Porous Materials, Eds. D. H. Everett and F. S. Stone, Academic Press, New York, 1958 (See also discussion following).
14. John Newman, I.E.C.Fund., 1968, 7, pp. 514-517.
15. N. Perrone and H. Liebowitz, Proc. of the First International Conf. on Fracture (Sendai, Japan), 1965, T. Yokobori, T. Kawasaki, and J. L. Swedlow, Eds., pp. 2065-2072.

Figure 1. Fluid flow in a propagating crack tip.

Figure 2. The boundary-layer function F, and its first derivative F', as a function of the position variable Y.

Figure 3. Model for Bubble Inside Crack.

Figure 4. Pressure from Hydrodynamics Compared to Equilibrium Pressure Outside Cavitation Bubble.

TECHNICAL INFORMATION DIVISION
LAWRENCE BERKELEY LABORATORY
UNIVERSITY OF CALIFORNIA
BERKELEY, CALIFORNIA 94720